Spin-polarized current-induced magnetization reversal in single nanowires

Derek Kelly,* Jean-Eric Wegrowe,† Trong-kha Truong, Xavier Hoffer, and Jean-Philippe Ansermet‡
Ecole Polytechnique Federale de Lausanne, CH-1015 Ecublens, Switzerland
(Received 13 September 2002; revised manuscript received 5 May 2003; published 17 October 2003)

Using electrochemical deposition, 6 μm long Ni nanowires, with typical diameters of the order of 80 nm, are grown in ion-track etched membranes. Electric contacts are established during the growth, allowing resistance measurements of a single magnetic wire. Whatever the angle of the applied magnetic field with the wire, the full loops of magnetoresistance of a nickel nanowire can be described quantitatively on the basis of anisotropic magnetoresistance of a uniform magnet, and exhibit a jump of the magnetization at the so-called switching field. Hybrid wires made half with nickel and half with a Co/Cu multilayer were also produced. The multilayer could be grown using either a single bath technique or a multiple bath setup, with the result of a different magnetic anisotropy in the Co layers. When the multilayer is made of an optimal number of layers, the two parts of the hybrid wire act as two resistances in series, having no magnetic interaction onto each other. In contrast, the action of a current pulse on the nickel magnetization is to provoke a switch, when injected before the unstable state of the hysteresis cycle has been reached. But the amount of applied field discrepancy where the current still has an effect is given by a measured value $\triangle H_{\max}$, which appears to be substantially dependent on the presence or not of a multilayer close enough to the nickel wire and on the orientation of the magnetization in the multilayer. The role of the multilayer's presence or state evidences the role of spin polarization in the current-induced switches of nickel. This is confirmed by measurements of the amplitude of $\triangle H_{\max}$ in homogeneous nickel wires that exclude spurious effects such as the induced oersted-field, heating, or a combination of the two to account for all the current-induced switches.

DOI: 10.1103/PhysRevB.68.134425 PACS number(s): 72.25.Ba, 72.25.Hg, 72.25.Pn

I. INTRODUCTION

Spin-transport in magnetic nanostructures is currently receiving increasing interest from the scientific community because of its importance in the design of new memory devices capable of maintaining the persistent increase in memory storage density and the accompanying need for information processing speed. Historically, as early as the 1950's, the coupling of conduction electrons to spin waves[1] was invoked in order to account for deviations from the simplest version of the two-current model that describes transport in metallic ferromagnets.[2] Ferromagnetic resonnance (FMR) experiments provided information on spin-flip scattering rates due to this coupling.[3] On the other hand, in the past two decades a lot of progress has been done in instrumental techniques providing physicists with capabilities of engineering structures on the nanometer scale. A size that is in principle small enough to allow the magnetization to remain uniform, making those samples magnetic single domain particles. Direct studies on spin-dependent scattering emerged from the first realizations of magnetic nanostructures and gave rise to the discovery of spin injection.[4,5] Studies of the exchange field coupling of a set of magnetic layers has brought to the discovery of giant magnetoresistance, a new property of spin-dependent electrical transport.[6–8] Tunnel,[9,10] ballistic magnetoresistance,[11] and domain wall scattering[12] are also concerned with the effect of a magnetic configuration on the conduction electrons. Recently the coupling of conduction electron spin to the exchange field was invoked to explain the electrical resistance of domain walls: the spin of the electrons follows almost but not exactly adiabatically the exchange field,[13] thus causing a slight spin-mixing[14] and consequently an increase in resistance.[15]

In the past decade or two, theoreticians pointed out the possibility of the converse effect of the current on the magnetization. Namely they predicted that spin-polarized currents of the order of 10^7 to $10^8 A/\mathrm{cm}^2$ excite spin waves[16–19] or propagate domain walls.[20] Recently it was also suggested that currents could be switching magnetic domains by longitudinal relaxation of the spin of the electrons.[21] In spin valves (injection into a magnet after spin polarization in a spin polarizer) it is thought that the injection of spins generates a torque,[22–27] an effective exchange interaction due to longitudinal spin accumulation,[28] or both torque and effective field due to transverse spin accumulation.[29] From the experimental point of view, first Berger *et al.*[30,31] have evidenced the action of a high current density on domain walls in thin films. Recently Garcia *et al.* provoked domains shifts causing magnetoresistance changes up to 300% in nickel nanocontacts by injection of ballistic electrons.[32,33] Tsoi *et al.* first inferred from *I-V* measurements that strong currents through point contacts into macroscopic Co/Cu multilayered thin films indeed excited spin waves,[34] later determined their high frequency nature, and suggested a transverse polarization configuration of the waves.[35] Further, magnon excitation in Fe/Cr/Fe trilayer films were directly observed by Rezende *et al.*[36] in the dynamic response of a multilayer, allowing to distinguish between the effects of spin injection and Oersted field on the magnetization. Theeuwen *et al.*[37] measured a reduction of the GMR ratio of a trilayer when traversed by an intense current in one sense but not if reversed, as well as the appearance of distinct high resistance GMR plateaus dependent on bias polarity and the sense of field sweep, possibly accounted for in part by the generation of incoherent magnons. Sun[38] attributed to momentum transfer onto ferromagnetic clusters the sudden resistance change in manganite trilayers. Ralph *et al.* observed

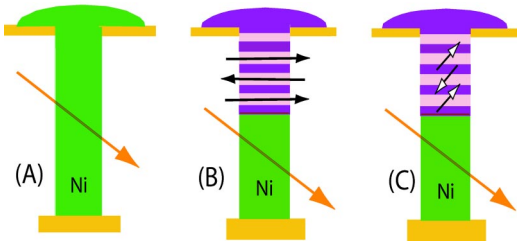

FIG. 1. (Color online). Three types of wires are used in this work: homogeneous nickel wires (A), hybrid wires with a nickel half-wire joined to a Co/Cu multilayer in which the Co layers are magnetized fully in-plane (B) or partially along the wire axis (C).

also a sudden resistivity enhancement beyond a threshold current in pillars[39] and multilayers[40]. The latter results and those of Theeuwen *et al.* were confirmed by Grollier *et al.*[41] although some discrepancy remains about the field dependance of the critical current. Recently, Weber *et al.* were able to distinguish precession due to exchange interaction and relaxation due to spin-dependent scattering of hot electrons flowing trough a thin magnetic film.[42]

Following the observation of current-induced magnetization switches in samples exhibiting a domain wall,[43] the experimental evidence of an effect of the spin polarization of conduction electrons on magnetization of a single magnet with high length-to-radius ratio, uniformly magnetized, has motivated the main effort of the present work. The spin-polarization effects were achieved by comparing the action of a high electric current density on the magnetization of a nickel segment in three types of wires: first, a nickel wire alone, second and third, two types of hybrid wires consisting of a nickel half wire preceded by a Co/Cu multilayer (Fig. 1). One type of hybrid has Co layers with anisotropy fully in plane of the layers and another type has Co layers with substantial anisotropy along the wire axis.

II. SAMPLE GROWTH

The wire synthesis is performed by electrochemical deposition in commercially available porous polycarbonate track etch membranes. Each membrane is covered on both sides with a gold layer of different thicknesses, thus providing microscopic contacts onto the wire. The thicker layer covers the narrowest pores and serves as working electrode. The thinner layer leaves most pores open in order to allow for the electrolyte to enter in them. Both layers are connected to a floating voltmeter that detects a potential drop as soon as the first wire connects between the two faces. At this point the voltage supply is stopped.[44] The thicker layer is also covered with silver paint, whose solvent prevents chemical growth in the thicker pores with the result of higher yield in getting single wire contacts, improvement of contact quality, and narrower distribution of wire diameters, with lower average.[46] Homogeneous nickel wires have a polycrystalline structure[47] and end with a contact on the thinner gold layer with a hemispherical shape revealed by an increase in deposition current[44] and observed by scanning electron microscopy.[48] The production of multilayers alternating Co and Cu layers of controllable thickness is achieved by modulating either the potential or by alternating the baths. The cobalt and copper layers are estimated to be 9 nm thick when the multilayer is grown from a single bath and 10 nm thick when the multilayer is grown from the multiple bath system. The thickness of a Co/Cu bilayer is known from the number of layers deposited, which is determined by the number of potential oscillations or bath changes before a contact is made between the two gold electrodes. The relative thickness of Co and Cu has been estimated by the change of number of layer with a change of layer deposition time for one the two materials.

Hybrid wires consist of a Co/Cu multilayer in series with a 3μm long nickel wire terminated by a copper contact. The nickel half-wire and the multilayer are separated by less than 10 nm of copper, usually 35 nm according to from the deposition time.

III. MAGNETIC CHARACTERIZATION

A. Multilayers

The magnetic behaviors of all samples were inferred from sets of $R(H)$ curves (resistance vs applied field) with different directions of field. Multilayers electrodeposited from a single bath containing both Co and Cu salts by varying the deposition potential[49] present distinguishable sets of resistance curves than multilayers grown by depositing alternatively from two different baths (Fig. 2). When the multilayer is electrodeposited from a single bath, the peak of the $R(H)$ curve is narrower in longitudinal field ($\Omega=0$) than in transverse field ($\Omega=90$). At a fixed value of applied field the resistance value is lower when the field is longitudinal, thus meaning that the layers are easier to align.

When the multilayer is electrodeposited from separate baths, the peaks of the $R(H)$ curves are nearly identical in longitudinal field than in transverse field, once the contribution of the anisotropic magnetoresistance is substracted from the total resistance. Both curves saturate at about the same value of field (they are parallel and nearly flat beyond ± 2 kOe). Second, the the difference between the curves for transverse field and longitudinal field increases approximately linearly as the GMR decreases, and remains constant when one of the curves becomes nearly flat. Indeed, the dipolar field approximation does account for the magnetic hysteresis behavior with the direction of the applied field in multilayers with layers thick enough for the dipolar interaction to be certainly dominant.[50]

The above observations allow to make qualitative estimation for both types of multilayers of their magnetic state at low field. The layers of single bath multilayers are easier to align in longitudinal field, so there must be a substantial anisotropy along the wire axis and at zero field the magnets are at least partially anti aligned along the wire axis since there is GMR. On the other hand, the curves of multiple bath multilayers for longitudinal and transverse field saturate at the same field. This implies that in this case the external field needs only to counter the dipolar anti alignment of the layers, but no anisotropy. The saturation field is much lower in this case than for single bath multilayers. Therefore no substantial anisotropy is present in the layers and only the dipolar

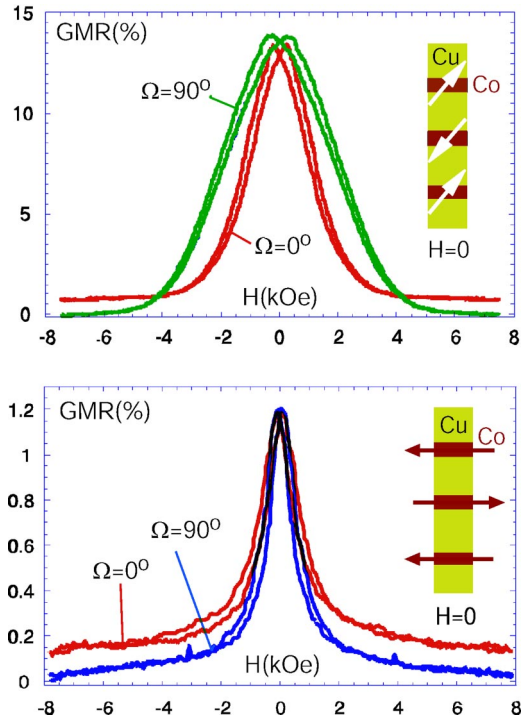

FIG. 2. (Color online). Two typical examples representative of $R(H)$ curves at room temperature. Top A $(Co9/Cu9)_{330}$ multilayer grown from a single bath, at longitudinal and transverse field with wire axis. Bottom: A $(Co9/Cu9)_{330}$ multilayer grown from separate baths, at longitudinal and transverse field with wire axis. In both cases the difference of resistance at $H_{max}=\pm 8$ kOe is due to the sum of AMR of all the cobalt layers.

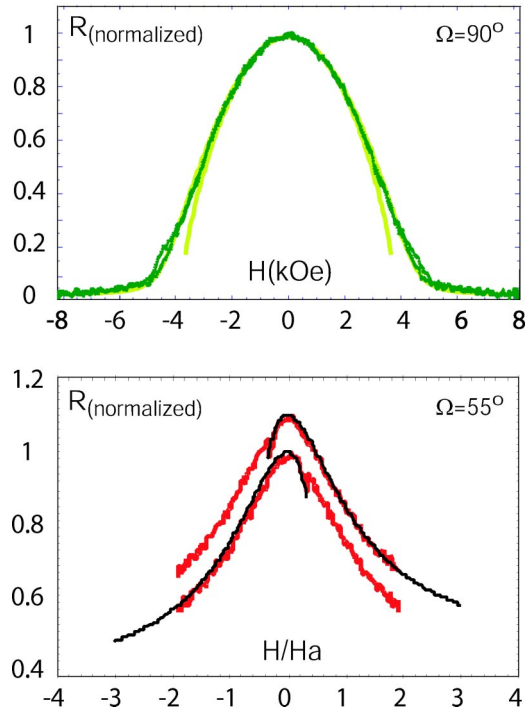

FIG. 3. (Color online). Normalized resistance hysteresis loops of r vs $H(h)$, measured at values of angle $\Omega=90°$ ($\Omega=55°$), where $h=H/H_a$ and $r_{AMR}(H)=[R(H)-R_\perp]/\triangle R_{AMR}$ with $\triangle R_{AMR}=R(0°)-R(90°)$ measured at $H=H_{max}$ ($H=H_{max}$ is a saturating field.) All experimental curves (dotted curves) are compared to the theoretical prediction (full lines) under uniform rotation of the magnetization. There is a good agreement at all values of field for every angle Ω.

field can determine the zero applied field configuration. Consequently, we expect the magnetizations in the multilayers fabricated with the multiple bath method to be in plane when the field is transverse and progressively out of plane when the field is longitudinal and changes from zero to ± 2 kOe.

B. Homogeneous wires

In homogeneous wires the hysteresis comprises two parts : a reversible part, and an irreversible jump at the so-called switching field. In many samples, data analysis reveals a uniform rotation of the magnetization (Fig. 3) in at least 98% of the wire's volume.[46] The jump in resistance is the irreversible transition between two uniformly magnetized states.[51,56] In some samples the reversible sections reveal the presence of a domain wall (Fig. 4). The domain wall is evidenced by a decrease in resistance before zero field is reached, by a non sharp resistance jump larger in size and arising at a field different that expected for uniform rotation of the magnetization.

C. Hybrids

Hybrid samples should exhibit— during a full half-loop in field (from one saturation to the opposite)— GMR and AMR and *one* jump that constitutes an increase in resistance, due to the irreversible switch of the nickel half wire. The contribution of AMR from the nickel half wire is estimated supposing a uniform rotation of magnetization in the resistance hysteresis. The geometry of the nickel half wire is here basically identical to that of a homogeneous nickel wire. Indeed, to the extent of what can be directly observed, the hysteresis of the nickel half wire in hybrid wires, is identical to that of homogeneous nickel wires.[52] Hence, the magnetoresistance curves of a hybrid sample will be plotted as

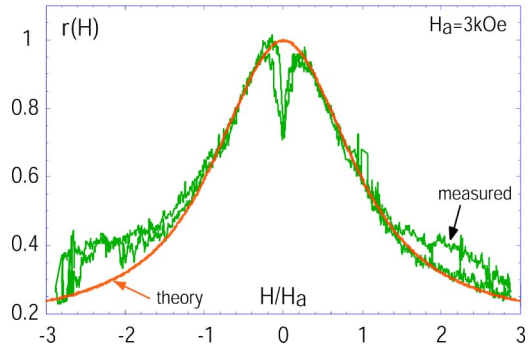

FIG. 4. (Color online). Normalized magnetoresistive curve of $r=(R-R_\perp)/\triangle R$ at $\Omega=69°$ of a homogeneous nickel wire. The solid line is the best curve obtained by comparison with the model of uniform rotation of magnetization. Note the large drop of resistance before $H=0$ is reached.

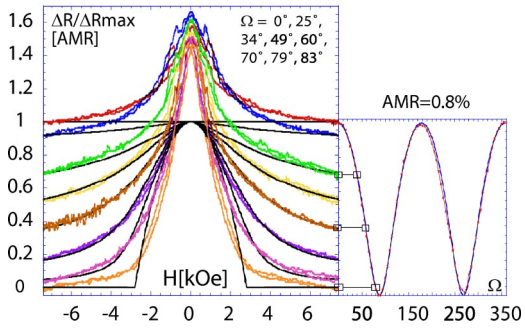

FIG. 5. (Color online). Experimental resistance hysteresis loops of $r_{\mathrm{AMR}}(H)=[R(H)-R_{\perp}]/\triangle R_{\mathrm{AMR}}$ with $\triangle R_{\mathrm{AMR}}=R(0°)-R(90°)$ measured at $H=H_{\mathrm{max}}$, for various angles of applied field. The curves are normalized with respect to the values of resistance at saturating field. All curves (dotted curves) are compared to the theoretical prediction under uniform rotation of the magnetization. The multilayer is grown by the multiple bath technique.

$r_{\mathrm{AMR}}(H)=[R(H)-R_{\perp}]/\triangle R_{\mathrm{AMR}}$ with $\triangle R_{\mathrm{AMR}}=R(0°)R(90°)$ measured at $H=H_{\mathrm{max}}$. It is justified by the fact that in completely multilayered wires the saturating field is reached at a field (<5 kOe) quite lower than $H=H_{\mathrm{max}}$ (>8 kOe). This allows us to estimate the contribution above 5 kOe as only due to the AMR of the nickel wire.

Experimentally, hybrid samples in which the multilayer was grown by the single bath technique, exhibit no jump of the nickel when the number of layers in the multilayer is above a number of 15 ± 2 cobalt layers (the latter number is valid for 10 nm thick cobalt layers) and only the AMR is observed when the number of cobalt layers in the multilayer is below the number of 15 ± 2 cobalt layers (of 10 nm thickness). All resistance features (GMR, AMR, and jump as increase in resistance), are visible in all the resistance curves when the multilayer has 15 ± 2 layers. Since multilayers grown from the multiple bath setup and filling the entire pore, i.e., 300 bilayers, exhibited a GMR of only 2% (compared to 25% in multilayers grown from a single bath), no hybrid wires were produced with only 15 Co layers. However, in hybrid samples grown from the multiple bath system, all resistance features are still present when the multilayer contains 150 layers of each material i.e. fills the whole second half of the pore. The fact that more layers can be grown in the latter case without hiding the features of the nickel half wire is thought to be due to the absence of anisotropy in the Co layers.

The resistance hysteresis at various angles of applied field for a hybrid sample with the multilayer made from separate baths is fairly well accounted for fields above 3 kOe, by the same procedure as for homogeneous wires (Fig. 5, the curve on the right-hand side is the AMR measured at an applied field of 8 kOe). The measured angular dependence of the switching field is also similar to the case of a homogeneous nickel wire. In particular, all samples exhibited a $H_{\mathrm{sw}}(\Omega)$ increasing with Ω from 0° to 90°. A selection of ten samples (nickel wires and nickel half-wires) illustrate the spread of these data (Fig. 6).

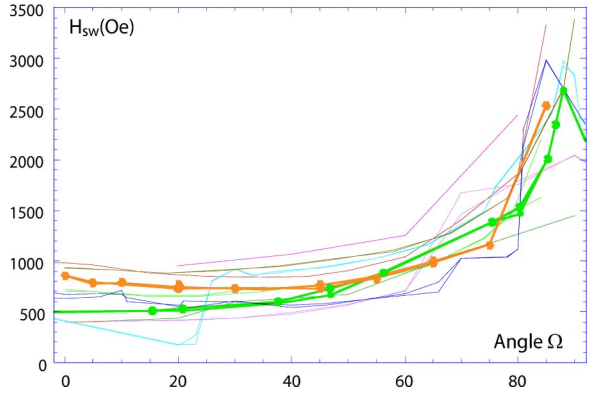

FIG. 6. (Color online). Angular dependence of the switching field in a selection of 10 nickel wires of diameters ranging between $r=10$ nm to $r=60$ nm. The two dotted bold lines represent a homogeneous wire (light gray dots) and a hybrid wire (dark gray dots).

IV. MEASUREMENTS ON HOMOGENEOUS WIRES

A. $\triangle H_{\mathrm{max}}$: a measure of the effect of the current on the magnetization

The magnetization irreversible switch in homogeneous ferromagnetic nanowires is shown to be triggered by the injection of a high current density of the order of $j_p=10^7\mathrm{A/cm}^2$ ($I_p\cong1$ mA in our wires) during 500 ns, when the applied field is below the value of the switching field by an amount $\triangle H_{\mathrm{max}}$ ranging from 100 to 700 Oe. The resistance jumps from a stable value at field H_p to the other stable state located at the same field on the half-loop reached from the opposite saturation (Fig. 7). H_p is the field value when the pulse is injected. Ω is the angle the applied field makes with the wire axis. Examples of initial stable states are sketched by the angle φ_0 between magnetization and the

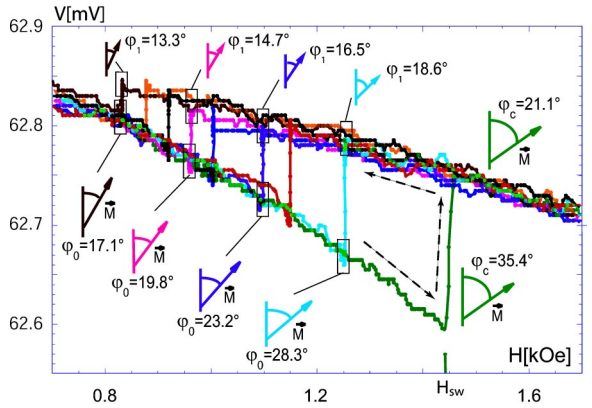

FIG. 7. (Color online). Current-induced transitions during a resistance hysteresis half-loop under an increasing field sweep at an angle of applied field of 65°. The increase in resistance occurs as the pulse is injected. The spontaneous jump occurs at $\varphi_c=35.4°$. Pulses of 2.6×10^7 A/cm^2 during 500 ns are injected before H_{sw}, provoking the jump. Four cases are sketched defined by φ_0. Pulse injection tilts the magnetization above φ_c, where it is no more stable. The dashed arrows sketch the path the magnetization would follow if monitored by a minor loop in field.

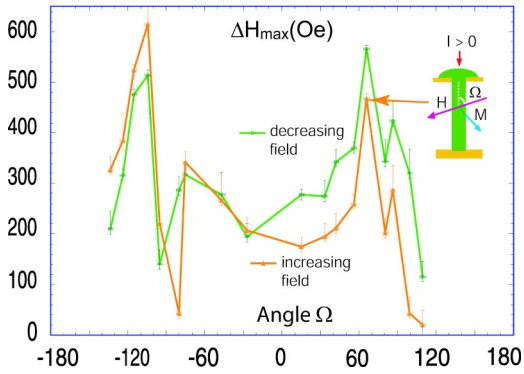

FIG. 8. (Color online). Angular dependence of the parameter $\triangle H_{\max}$ for a current pulse of 1 mA (about 1.5×10^7 [A/cm^2]) for increasing or decreasing field.

wire axis. Examples of final stable states are sketched by the angle φ_1 the magnetization makes with the wire axis after pulse injection. When no pulse is injected, the switch occurs at field H_{sw}.

The most important feature shown in Fig. 7 is that for all angles and intensity of applied field, the final states after the current pulse injection are located on the same hysteresis curve corresponding to the opposite field sweep (associated to uniform configurations) as for the switch without current pulse injection. Thus all happens *as if* the magnetization affected by a high-intensity current-density actually follows (path sketched by dashed arrows) the same path it would follow under the influence of a minor loop of applied field from H_p to $H_{\mathrm{sw}}+H_\epsilon$ (with H_ϵ small enough) and back to H_p.[53] The magnetization rotates up to the regular unstable state, switches, and rotates back to the stable state associated to the applied field H_p. The pulses provoke the jump in resistance until the difference defined as $\triangle H=|H\text{-}H_{\mathrm{sw}}|$ reaches a value $\triangle H_{\max}$ above which they do not. In a homogeneous wire with uniform magnetization, each resistance value along a half loop corresponds to one and only one magnetic state, i.e., Ω univokely defines φ, the angle of the magnetization with the current flow. Hence, the pulse does not create any new (i.e., nonuniform) magnetic state after the injection. Consequently, the current-induced jumps *can* be modeled as the magnetization of the nickel wire following the same path it would under the influence of a minor loop in applied field.[53]

The increasing field hysteresis half loop is repeated for other angles Ω of applied field with wire axis. The same measurements are repeated then for decreasing field ramp (Fig. 8). The injected high intensity current is always *positive*, i.e., the electrons flow goes first through the hemispherical contact. $\triangle H_{\max}(\Omega)$ has a minimum at a value Ω_0 in the interval $\mp20°$, increases with $\triangle\Omega$ ($\Omega=\Omega_0\pm\triangle\Omega$). A maximum value is reached at a value in the interval $[\Omega_0+70°;\ \Omega_0+90°]$. A second maximum is reached at an angle symmetric by 180° in the interval $[\Omega_0-70°;\ \Omega_0-90°]$. This global feature is always present in homogeneous nickel wires, whatever their characteristics are (diameter, magnetic hardness, uniform rotation in the reversible sections, or presence of a domain wall).

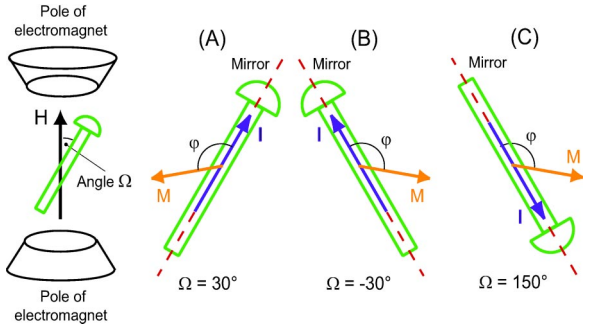

FIG. 9. (Color online). Three different angles of the wire with the applied field, for which identical values of $\triangle H_{\max}$ are expected because a symmetry with a mirror parallel to the wire axis keeps the wire unchanged as well as the relative orientation between $\vec{M}$ and $\vec{I}$ (from A to B) or between $\vec{M}$ and the sl axis of I (from A to C).

The scattering of the points on a curve must be distinguished from the uncertainty in the determination of a $\triangle H_{\max}$. All values of $\triangle H_{\max}$ are reproducible within the error bars. The only events that are accepted for the determination of $\triangle H_{\max}$ are jumps in resistance that produce instantaneously a transition between the two states determined by the hysteresis without pulse injection (in the sense of a quasistatic measurements, instantaneously means less than 100 ms).

B. Symmetries in uniformly magnetized wires

The curves $\triangle H_{\max}(\Omega)$ present features with Ω which requires to distinguish between homogeneous wires that are monodomain, whose hysteresis loops are in agreement with an uniform rotation of magnetization, and those wires who exhibit the presence of a domain wall. Some features could arise from purely geometrical factors: the wire's axis is identical to the current flow axis, but the magnetic probe consists of the wire *and* the contacts at its ends. For ideal contacts, the magnet has an axial symmetry. In terms of angle Ω in the setup's plane of rotation, this axial symmetry means the magnet has a mirror symmetry (the mirror is the plane along the wire axis and perpendicular to the plane of rotation of the field) (Fig. 9).

We begin with the wires of resistance loops in agreement with a uniform rotation of magnetization.

For a fixed sense of current flow, there appear some symmetries of $\triangle H_{\max}$ with Ω. First, $\triangle H_{\max}(\Omega)$ is symmetric around the minima, i.e., $\triangle H_{\max}(\Omega_0+\triangle\Omega)=\triangle H_{\max}(\Omega_0-\triangle\Omega)$. Second, $\triangle H_{\max}(\Omega)$ is symmetric around the maxima. Consequently $\triangle H_{\max}(\Omega)$ is identical for opposite field half loops (Fig. 8).

$\triangle H_{\max}(\Omega)$ would be expected to be exactly symmetric around the minima (maxima) and the minima be at $\Omega=\Omega_0=0°$ ($\Omega=\pm90°$) but which is only approximately the case. The slight influence the magnetic contact has on the observed values of $\triangle H_{\max}$ can be tested by growing a nickel wire, stopping the electrodeposition just before a contact is made and then making the contact with a copper electrolyte. Such a wire is free of coupling to an undesired additional magnet and indeed the curves of $\triangle H_{\max}$ for increasing and

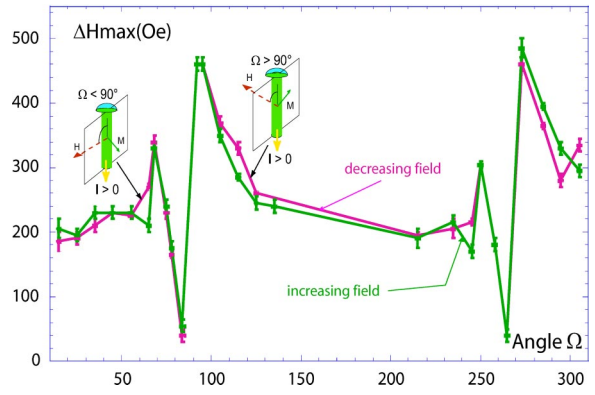

FIG. 10. (Color online). Dependence with respect to Ω of the $\triangle H_{\max}$ associated to the pulse injection in a nickel wire with a Cu contact.

decreasing field appear superimposed and centered around $\Omega = 180°$ (Fig. 10). (An additional feature is the drop of $\triangle H_{\max}$ for Ω very close to 90°).

For monodomain nickel wires, the values of $\triangle H_{\max}$ for one sense of current flow are always lower than for the other, whatever Ω, the sense of applied field ramp remaining the same (Fig. 11). In addition, $\triangle H_{\max}$ did not change with a reversal of field ramp. Thus, for monodomain nickel wires the sign of variation of $\triangle H_{\max}$ with a reversal of current flow is the same whatever the sense of field ramp.

The symmetry about 0° means that the effect depends only on $|\Omega|$, i.e., on $|\varphi|$. Two field sweeps symmetric with Ω, i.e., for $\Omega = 0° \pm \triangle\Omega$, will bring the magnetization also in symmetric directions, i.e., identical $|\varphi|$. The symmetry about ±90° (i.e., for two sweeps with $\Omega = 90° \pm \triangle\Omega$)means that the effect depends only on the angle between the magnetization and the *axis* of current, whatever the sl sense of flow. Both symmetries (around 0° and around ±90°) are expected whatever the cause of the effect, as long as the magnet is symmetric with the *axis* of current flow. But for the latter in addition, the fact that such a symmetry around $\Omega = 90°$ is observed, means that the effect *is* independent of the sign of the velocity of the electrons. Note the orientation of the Oersted field does depend on the sign of the electrons

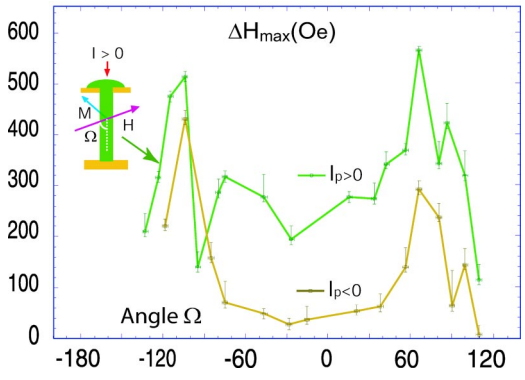

FIG. 11. (Color online). Angular dependence of the $\triangle H_{\max}$ for a current pulse of ±1 mA (*about* 1.5×10^7[A/cm^2]) injected into a homogeneous nickel wire exhibiting uniform rotation of magnetization when applying a decreasing field loop.

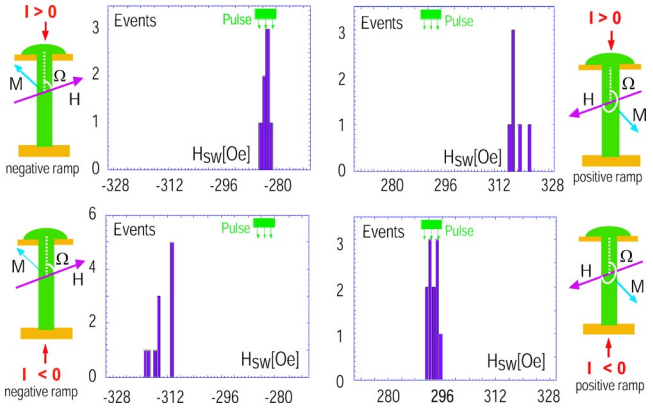

FIG. 12. (Color online). Histograms of the number of switches occurring at a field *H*, when a pulse is injected at H_p into a homogeneous nickel wire exhibiting the presence of a domain wall when applying a field loop. The applied field at saturation at the start of the field ramp, a representation of the average direction of magnetization just prior to the switch, and the current flow sense with relative orientations are sketched next to each cell.

velocity. On the other hand this does not exclude at all asymmetric effects with the sense of current flow since e.g. the spin-polarization of the current may change with the sense of current flow.[54]

A consequence of the above two symmetries and the asymmetry is that, when rotating the whole external system (i.e., field *and* current flow) except the wire itself, the curve $\triangle H_{\max}(\Omega)$ is not conserved. So the asymmetry of $\triangle H_{\max}$ must be linked to a structural geometric asymmetry of the wire. Indeed, the two contacts are not identical, thus there is a magnetic asymmetry. Considering the ensemble of the *two* magnetic contacts as the polarizing source, a change of the *net* spin polarization at the tips of the wires when changing the sense of current flow could reflect that asymmetry.

C. Symmetries in wires containing a domain wall

A different picture arises when we consider the homogeneous nickel wires, the resistance loops of which exhibit the presence of a domain wall (Fig. 4). In those wires asymmetries were observed with reversal (i.e., change in sign) of either injected current-pulse flow or sense of applied field ramp but no variation of $\triangle H_{\max}$ with reversal of both. For one sense of current the values of $\triangle H_{\max}$ are lower in one range of angle Ω, but in another range the values of $\triangle H_{\max}$ are higher compared to the other sense of current: the sign of variation of $\triangle H_{\max}$ with a reversal of current flow is different if the field ramp is positive or negative. The sign of variation of $\triangle H_{\max}$ with a reversal of field ramp is opposite if the current is positive or negative. The variation of $\triangle H_{\max}$ is of about ≃40 Oe when the field ramp is reversed and the samples that showed this type of asymmetry exhibited low values for $\triangle H_{\max}$.

A consequence of the *asymmetry* observed in wires *containing a domain wall* is that $\triangle H_{\max}$ is conserved when both the applied field and the current sense are reversed (Fig. 12). Thus the effect here *does* depend on the sense of velocity of

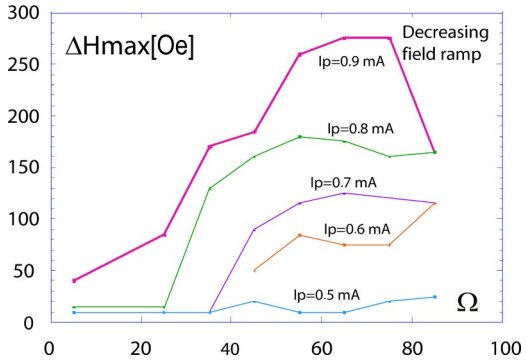

FIG. 13. (Color online). Measurements of $\triangle H_{\max}(\Omega)$ with a wire of radius $r \simeq 10$ nm.

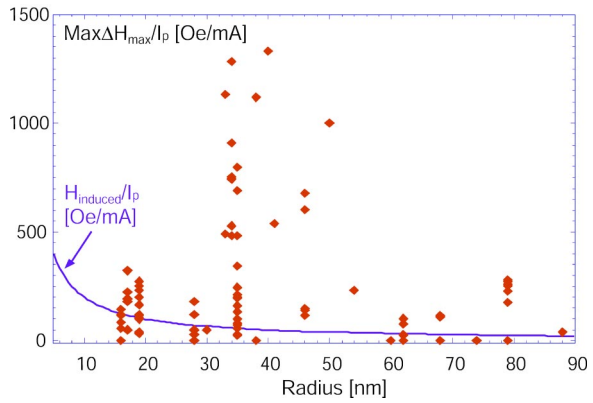

FIG. 14. (Color online). $\max\triangle H_{\max}/I_p$ as a function of the radius of the wire it was measured in. The radii are minimal boundaries i.e. they were estimated neglecting the presence of a contact resistance. Some dots aligned vertically are relative to the same wire.

the electrons with respect to the orientation of magnetization. So although an effect of the spin-polarization of the current may still be present,[43] another effect adds up, giving rise to the asymmetry described in Fig. 12. This type of asymmetry can be accounted for by the induced field, because $\triangle H_{max} \approx H_{\rm ind}$ and $\triangle H_{\rm ind}$ has a good geometry for acting on a domain wall.[33] Also, the orientation of $H_{\rm ind}$ with the magnetization inside the domain wall changes when the sense of only the field ramp or the current flow is reversed and a $\triangle H_{\max}$ originating from the Oersted field is conserved when everything (including the orientation of the magnetization) is rotated by 180°, except the wire itself. This type of *symmetry* is expected when the wire is perfectly cylindrical and the net spin polarization is not current-sense dependent.

V. SPIN-POLARIZATION EFFECTS VERSUS OTHER CURRENT-INDUCED EFFECTS

The effect of the current, as measured by $\triangle H_{\max}$, was studied as a function of the radius. Spurious causes generating the observed $\triangle H_{\max}$ in homogeneous wires *where no domain wall is present* could be ruled out: Joule heating, the current-induced Oersted field amplitude, the gradient of the Oersted field or a combination of them.

The angular dependence of $\triangle H_{\max}$ in membranes with pores of radius $r \leqslant 15$ nm (Fig. 13) appears to be similar to the angular dependence in membranes with pores of radius 20 nm$\leqslant r \leqslant$50 nm. $\triangle H_{\max}$ takes nearly identical values for decreasing and increasing field sweeps and $\triangle H_{\max}(\Omega)$ increases with Ω, and drops near 90°.

The striking result here is that the *intensity* of current required to trigger the switch is independent of the radius (Fig. 13). The minimum current required to trigger an effect does not scale neither with the increase of the current-induced field nor with the Joule heating. Although in some cases these other current-induced effects are present in non-negligible amounts, they never *fully* account for the data.

Prior to analysis, a new parameter $\max\triangle H_{\max}$ common to every sample must be introduced. Considering the possibility that the angular dependence of one or the other spurious current-induced effects varies with the radius of the wire, a comparison between samples of $\triangle H_{\max}$ at the same angle may not be relevant. $\max\triangle H_{\max}$ is defined as the highest $\triangle H_{\max}$ observable in a sample for a fixed intensity I_p of current-pulse excitation.

To study the dependence of $\max\Delta H_{\max}$ with radius r, one should take into account the possible dependence on radius of magnetic parameters such as the total anisotropy field H_a or the magnetic hardness D. H_a for wires with different radii can be estimated from the fits of $R(H,\Omega)$ or from $H_{\rm sw}(\Omega)$.[46] No clear increase of H_a was observed as the radius was decreased. Rather, the samples with radii lower than 35 nm had lower H_a than those with radii higher than 35 nm. The magnetic hardness is defined as

$$D = \left(\frac{r_0}{r}\right)^2$$

where k is a dimensionless geometry-dependent factor equal to 1.079 for an infinite cylinder.[45] r_0 is a material-dependent parameter linked to the quantum exchange constant and can be taken as $r_0 \approx 20$ nm in Ni and $r_0 \approx 7$ nm in Co. The magnetic hardness is to be taken into account only when the switching breaks the uniformity of the magnetization. (It is the case for the induced field, $H_{\rm ind}$, but not in a model where the magnetization rotates uniformly during the switch.)

A. Observed current-induced effects versus current-induced Oersted field effects

The magnetic field induced by the current I is poloidal. Its value inside of the wire at a distance r_i of the wire axis is given by

$$\frac{H_{\rm ind}}{I_p} = \frac{r_i}{2\pi r^2} \tag{1}$$

which is maximal on the surface of the wire ($r_i = r$). Let us assume the poloidal field is now the cause of the current-induced switch, i.e., $\max\triangle H_{\max}$ is simply proportional to $H_{\rm ind}$. Thus the value $(\max\triangle H_{\max})/I_p$ should be inversely proportional to the wire radius and a distribution for different r and I_p should be placed on a *single* curve. It is not the case,

and the distribution of experimental values $\max\Delta H_{\max}/I_p$ turns out to have a maximum in the range of $r=35$ nm to $r=50$ nm (Fig. 14).

The magnetic hardness $D\propto r^{-2}$ and $H_{\text{ind}}\propto r^{-1}$, thus $\max\Delta H_{\max}/I_p$ should still be monotonic with r and all values should be placed on a single curve. The observed distribution does not allow one to identify $\max\Delta H_{\max}/I_p$ with an effect of H_{ind}. This does not exclude, however, H_{ind} from partially contributing to the current-induced switching, and this contribution from depending on r or Ω. A possible route to get the relative contribution of H_{ind} to $\Delta H_{\max}$ could be to compare H_{ind} with $\Delta(H_{\text{int}})_{\max}$, where $\Delta(H_{\text{int}})_{\max}$ is defined as $\Delta H_{\max}$ but using the internal field H_{int}. The internal field yields

$$H_{\text{int}}(\Omega,\varphi)=H(\Omega)-H_{\text{dem}}(\Omega,\varphi)$$
$$=H(\Omega)-2\pi M_s\sin\varphi(H,\Omega). \quad (2)$$

H_{dem} is the demagnetizing field, M_s is the saturation magnetization, and φ is obtained from the fits of $r(h)$ by minimizing the sum of all energy terms (including the magnetostatic energy) assuming uniform rotation of the magnetization.[46] Thus

$$H_{\text{int}}^2=(H\sin\Omega-2\pi M_s\varphi)^2+(H\cos\Omega)^2. \quad (3)$$

The angle $\phi(H,\Omega)$ that H_{int} makes with the wire axis is such that $\Phi<\Omega$ and $|\Omega-\phi|\to 0$ with increasing H.

For example, at $\Omega=0°$, 60°, 65°, 80°, 90° with $H_{\text{sw}}=900$, 1000, 1400, 1500, 2700 Oe and $\Delta H_{\max}=200$, 450, 600, 600, 100 Oe, $\Delta(H_{\text{int}})_{\max}$ yields 200, 260, 355, 150, 0 Oe. However, a link between $\Delta(H_{\text{int}})_{\max}$ and H_{ind} remains unclear since no theory exists. Indeed, the switching process under the action of a homogeneous field is still a topic of recent investigations.[46,51]

The spatial distribution of H_{ind} is axial and favors a curling type of reversal. One would expect the effect of H_{ind} to be strongest when the magnetization is still parallel to the wire axis prior to the current pulse injection, i.e., H_{ind} should act strongest at $\Omega=0°$, which is not the case even when $\Delta(H_{\text{int}})_{\max}$ is considered. $\Delta H_{\max}(\Omega=0°)$ can be directly compared to H_{ind} since $H^{\text{dem}}(\Omega=0°)\approx 0$ Oe. $\Delta H_{\max}(\Omega=0°)$ can take values up to 250 Oe in homogeneous wires where $H_{\text{ind}}\approx 30$ Oe.

The gradient of Oersted field generated during pulse injection is

$$\nabla H_{\text{ind}}=\frac{I_p}{2\pi r^2}=\frac{j_p}{2} \quad (4)$$

and has to be compared to

$$\nabla 4\pi M_{\text{wall}}\cong\frac{4\pi M_s}{d_{\text{wall}}}, \quad (5)$$

where $\nabla 4\pi M_{\text{wall}}$ is the field gradient inside the wall and d_{wall} is the typical domain wall thickness. $4\pi M_s$ is the local field associated to the saturated magnetization on one side of the wall and it is $-4\pi M_s$ on the other side. It can be seen in many samples that the values of $\nabla B/\nabla M_{\text{wall}}$ are too low by more than one order of magnitude for the gradient of the Oersted field to be able to generate a domain wall and thus possibly trigger the magnetic switch. Thus from the ratios of $\nabla B/\nabla M_{\text{wall}}$, ∇B cannot account for the amplitude of $\max\triangle H_{\max}$ in the range of wire radii investigated. It may still be that the current-induced Oersted field itself or its gradient may act locally in a region where the creation of an inhomogeneity is facilitated, but then there is little reason why a homogeneous wire always has the same angular dependance for $\triangle H_{\max}$, and the influence of inhomogeneities are likely to have been included already in the value of H_{sw}.

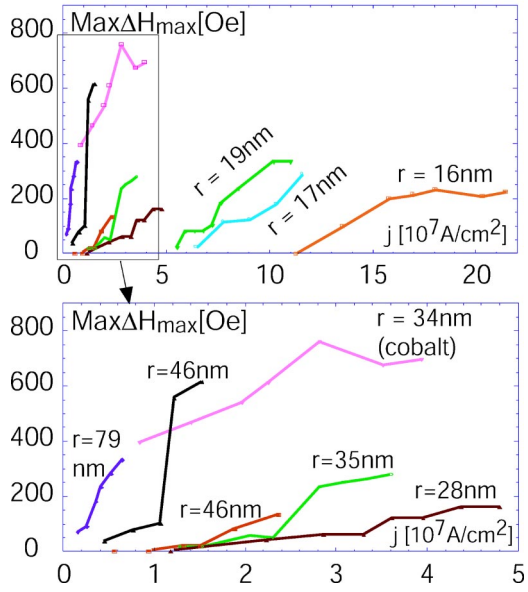

FIG. 15. (Color online). Dependence in radius r and current pulse density j_p of the parameter $\max\triangle H\max$ is given by curves of $\max\triangle H_{\max}$ as a function of (j_p) using the radius of the associated wire as a parameter. $\text{Max}\triangle H_{max}(j_p)$(top) shows two regimes of current density needed to reach a fixed value of $\max\triangle H_{\max}$. One regime is in the decade $j_p=10^7$ A/cm^2 of current density needed to trigger the reversal. The other regime is in the range $j_p=10^8$ A/cm^2. The regime of $\max\triangle H_{max}(j_p)$ for lower densities (curves on the left the graph) is zoomed (bottom). The zoom shows that in the regime of the decade $j_p=10^7$ A/cm^2 (lower densities), a monotonic radius dependence is still present. All samples are nickel wires except one made of cobalt.

B. Observed current-induced effects versus Joule heating effects

The heating due to the current pulse has been determined experimentally by resistance measurements.[55] An upper bound can be provided by a simple model. Let us consider the most extreme case of heating, where the Joule power is injected in the center of the wire by a pulse of constant amplitude. The heat reservoirs are the leads contacted to the tips of the wire (surface πr^2; distance$=L/2$, where $L=6$ μm$=$wire length), and the polycarbonate surrounding the wire a certain thickness away (distance $\delta=500$ nm, boundary surface $2\pi rL$). The thermal conductivity in the

wire and in the membrane are respectively κ_{Ni} and κ_{memb}. R is the wire resistance and I_p is the injected current. In the stationary regime

$$RI_p^2=\rho L\pi r^2 j_p^2=\triangle T\left(\kappa_{Ni}\frac{4\pi r^2}{L}+\kappa_{\mathrm{memb}}\frac{2\pi rL}{\delta}\right). \quad (6)$$

The change in coercive field $\triangle H_c$ due to a change $\triangle T$ in temperature has been measured experimentally in magnetometry of many wires[55] as

$$\triangle H_c=n\triangle T, \quad (7)$$

where $n=3$ [Oe/K]. In first approximation, one can take $\triangle H_c=\triangle H_{\mathrm{sw}}$. So let us assume $\triangle H_{\mathrm{sw}}$ is due to the Joule heating : $3\triangle T=\max\triangle H_{\max}$. A numerical estimation[43] has already suggested that $n\triangle T\ll\triangle H_{\max}$.

In order to check for the radius dependence of $\max\triangle H_{\max}$, Eq. (4) can be simplified by neglecting dissipation in the polymer. Considering cooling only through the leads, one gets for a nickel wire

$$\triangle T=\frac{\rho L^2 j_p^2}{4\kappa_{\mathrm{Ni}}} \quad (8)$$

and κ_{Ni} must be replaced by κ_{Co} for a cobalt wire.

$\mathrm{Max}\triangle H_{\max}$ should then be independent of radius at fixed j_p, which is definitely not the case (Fig. 15 top). Considering only cooling into the membrane, one gets

$$\triangle T=\frac{\rho\delta r j_p^2}{2\kappa_{\mathrm{memb}}}. \quad (9)$$

For a fixed $\triangle T$, i.e., fixed $\max\triangle H_{\max}$, the radius should decrease as j_p^{-2}. The distribution of the $\max\triangle H_{\max}(j_p)$ (Fig. 15 top) clearly does not support this either.

From the above it can be concluded from the radius dependence of $\max\triangle H_{\max}(j_p)$or $\max\triangle H_{\max}(I_p)$, that it is not possible to account for $\max\triangle H_{\max}$ of all the different samples in the framework of Joule heating. A direct confirmation of the estimated values of heating comes from the measurement of $\triangle R/R$ in a dc measurement where it could be seen that a current of 2 mA (highest intensity ever used in this work) produces a heating of 20 K, hence a $\triangle H_{\max}$ of 60 Oe, much too low to account for the different values of $\triangle H_{\max}$.[56] Finally, another confirmation of this conclusion comes from time-resolved experiments that have shown that a high current above a threshold intensity induces a non thermal contribution to the magnetization switching. The current appears to lower the energy barrier for switching.[57,58]

C. Dependence on the material

The cobalt sample in Fig. 15 is a cobalt wire that exhibits a $\max\triangle H_{\max}(I_p)$ with much higher values than all other samples in Fig. 15, made of nickel. Although the anisotropy field is found higher in cobalt than in nickel, $\max\triangle H_{\max}(I_p)$ is higher in a cobalt wire. One would expect of effects like heating or the Oersted-field to have at fixed current intensity and wire radius a reduced influence on $\max\Delta H_{\max}(I_p)$. On the other hand, the magnetic hardness is lower than in nickel allowing for more or smaller magnetic inhomogeneities. The uniformity of the magnetization in a cobalt wire cannot be proved within the precision of our fits of $r(h)$ assuming uniform rotation of the magnetization. Thus a different material could modify the mechanism and relative contribution of the different current-induced effects. More investigations are required to make conclusions from a change in material.

VI. NICKEL WIRE PRECEDED BY A SPIN POLARIZER

The purpose of the comparison of the current-induced effect between a nickel wire preceded by a multilayer and a nickel wire without a multilayer, is to generate an asymmetry of the current-induced effect on the nickel probe by building controllably an asymmetric magnetic structure. Thus we compare first a nickel wire with a hybrid wire made of a nickel half wire and a Co/Cu multilayer produced with the multiple baths method. Since the Co/Cu multilayer exhibits GMR, we can think of it as an injector of spin-polarized electrons. Thus the interface between Ni and the multilayer gives rise to spin accumulation sites in Ni.

A. Measurements

The striking result is the observation that for hybrid samples the angular dependence of $\triangle H_{\max}$ is shifted by 90° compared to that of the homogeneous nickel wire (Fig. 16). The features of $\Delta H_{\max}(\Omega)$ for scatter appear however somewhat more complex for the hybrid wires. In these hybrid samples $\triangle H_{\max}(\Omega)$ is independent of the sense of current flow and sense of field ramp. Nevertheless, the maxima of $\Delta H_{\max}(\Omega)$ for the homogeneous nickel wire occur at angles Ω where $\Delta H_{\max}(\Omega)$ for the hybrid wire is low.

B. Discussion

We have shown that the multilayer does not affect the magnetization hysteresis of the nickel and that the resistance hysteresis is similar in a nickel half-wire than in a homogeneous nickel wire. H_{ind} should have the same effect on both nickel probes. However, $\Delta H_{\max}(\Omega=0°)\approx 400$ Oe but $H_{\mathrm{ind}}\approx 65$ Oe. Also, $\Delta H_{\max}(\Omega=0°)$ in the hybrid is larger than in the homogeneous wire (400 Oe, resp. 200 Oe) although the magnetic hardness is increased since the radius is reduced (35 nm, resp. 46 nm). What does change is the magnetic environment where the spins enter the nickel probe. Hence, $\Delta H_{\max}$ changes when the spin polarization of the current at the tips of the nickel probe changes. From the magnetic characterization, we can conclude that the effect of the current is largest when the magnetization of the Co layers is perpendicular to the magnetization orientation in the nickel. Indeed we found that the magnetization in the multilayers made from multiple baths were in the plane of the layers at low field, whatever the direction of applied field. (When the field is parallel to the wire, the switch in Ni occurs below an applied field of 900 Oe.) As the current flows through the multilayer, the spin polarization is also perpendicular to the wire axis provided the spin polarization fully aligns with the magnetization. Thus our observation (Fig. 16) implies that

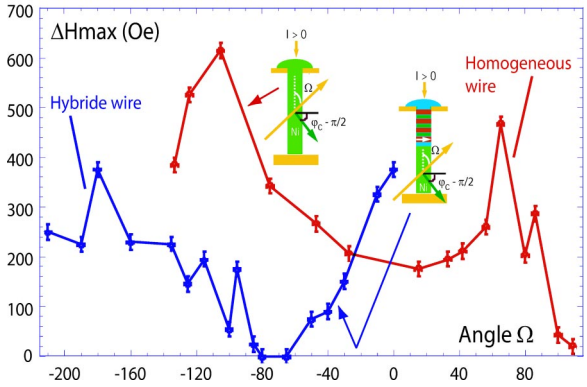

FIG. 16. (Color online). Angular dependence of the parameter $\triangle H_{\max}$ for a pulsed current of 1.6 mA (about 4.1×10^{7}[A/cm^2]). φ_c represents the angle of wire axis with magnetization just prior to the switch.

the effect of current is largest when the spin polarization of the current entering the nickel is perpendicular to the nickel magnetization orientation. In the framework of spin-polarized current induced effects, the symmetry of the current-induced effect with the sense of applied field can be understood from a particular symmetry of the system with the applied field. The relative angle $\triangle\varphi$ between the magnetization in the cobalt layer nearest to the nickel and the magnetization in the nickel half wire remains identical if the field is shifted to a direction symmetric with the axis of the wire [compare (1) and (3) in Fig. 17]. That relative angle also remains identical when the applied field is at an angle 90° $\pm\triangle\Omega$ with the wire axis [compare (1) and (4) in Fig. 17] or when the sense of field is reversed, i.e., rotated by 180° [compare (1) and (2) in Fig. 17]. In every case the direction of the magnetization in the Co layer lies between the direction of the magnetization in nickel and the direction of the applied field. The shift in 90° of $\triangle H_{\max}(\Omega)$ between the hybrid and the homogeneous samples occurs whatever the sense of current implies the multilayer fixes the spin polarization near the tip of the nickel half wire regardless of the sense of current.

C. Control experiments

Two further experimental observations have been made that link the current-induced effect to the relative orientation of the spin flow and the magnetization. First, in a hybrid sample in which the non magnetic spacer is much longer (Cu spacer of 200 μm) than the spin diffusion length $\triangle H_{\max}(\Omega)$ is the same as in a homogeneous wire (Fig. 18).

Second, measurements of $\triangle H_{\max}(\Omega)$ were also performed on hybrid wires, in which the multilayer part was produced with the single bath technique (Fig. 19). In this case a gradual increase of $\triangle H_{\max}$ up to above 1400 Oe is observed between $\Omega=0°$ and $\Omega=90°$. The magnetic characterization had shown that a multilayer grown from a single electrolytic bath has a total anisotropy parallel to wire, identical to the case of the magnetization in a homogeneous wire. Thus, the conduction electrons could get polarized in similar way in this multilayer or in a homogeneous wire and one would expect a similar angular dependence for $\triangle H_{\max}(\Omega)$. No dependence of $\triangle H_{\max}(\Omega)$ with the sense of the injected current or the sense of the applied field ramp were found in such hybrid wires, either.

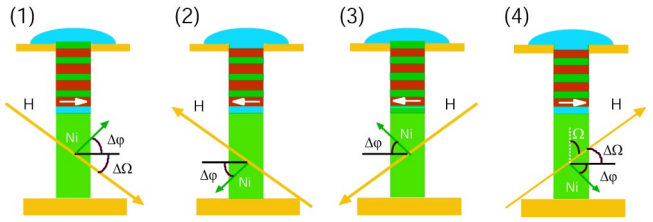

FIG. 17. (Color online). Symmetries of the magnetic configuration in the hybrid sample with respect to the direction of the applied field.

D. Quantitative analysis

For a quantitative analysis of the observed data in the framework of spin-polarized current action on magnetization it is convenient to start from the Landau-Lifschitz-Gilbert (LLG) equation for the motion of magnetization and generalize it to include the presence of a current.[21] This can be accomplished by adding a contribution $\vec{f}(\vec{e}_p, \vec{M})$ dependent on the unit vector $\vec{e}_p$ which gives the direction of the spin polarization of the incident current, and the magnetization state $\vec{M}$. In a first common approach it is assumed that this additional contribution is proportional to the spin-carrier flow entering the magnet $\vec{\nu}I_p/e$ ($\vec{\nu}$ is a unit vector normal to the wire's surface), and to the magnetic charge of each carrier $g\mu_B$ and its dependence on the magnetization state is weak.[16] The modified LLG equation is then

$$\frac{d\vec{M}}{dt} \approx -g'M_s\left(\vec{M}\times\frac{dV}{d\vec{M}}\right)-h'\left(\vec{M}\times\frac{dV}{d\vec{M}}\right)\times\vec{M}+f(\vec{e}_p)\frac{g\mu_B I_p}{e}, \tag{10}$$

where I_p is the injected current pulse intensity, e is the electric charge of the electron, g is the Landé factor, μ_B is the Bohr magneton. $\vec{M}$ is the total magnetization. The phenomenological parameters h' and g' (Ref. 59) are linked to the gyromagnetic ratio γ and the Gilbert damping coefficient α by the relation $h'=\gamma\alpha/(1+\alpha^2)M_s$ and $g'=\gamma/(1+\alpha^2)M_s$. The contribution of outgoing electrons to Eq. (10) is negligible since the loss of spin polarization occurs outside the magnet's volume, i.e., is randomly dissipated by electrons not coupled by the exchange interaction.

The first and second terms in the right hand side of Eq. (8) are transverse relaxation modes. They are, respectively, the precession term and the damping term. The third term in the right-hand side is the spin injection due to spin polarized conduction electrons, which may modify a transverse mode (this conserves $\|\vec{M}\|$) or be the source of a longitudinal relaxation of the spins (dynamically changes $\|\vec{M}\|$).

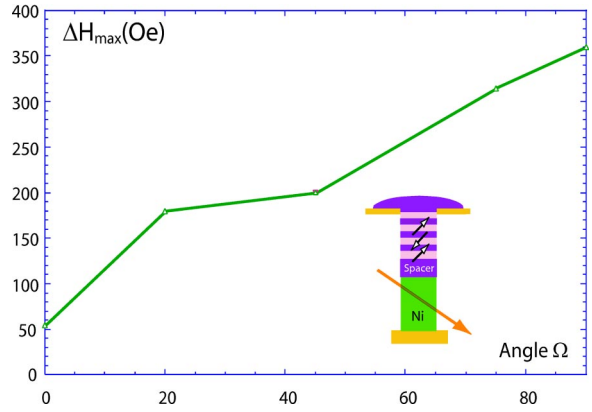

FIG. 18. (Color online). Measured angular dependence of the parameter $\Delta H_{\max}$ for a hybrid wire containing a nickel half-wire and a Co/Cu multilayer separated by a Cu spacer of 200 μm grown with the single bath technique. The sample exhibits well separated GMR and AMR when applying a loop in field.

The unspecified function $\vec{f}$ introduced in Eq. (8) depends on the chosen model. Most models to date yield a torque on the magnetization (parallel or antiparallel to the damping). However, those models[22–29] assume an incident spin-polarized current onto a thin magnetic layer and the torque generates essentially an in-plane rotation of the magnetization. In the present context of spin-polarized current-induced effect in a long uniformly magnetized nickel wire where the magnetization along the wire axis changes, Bazaliy's model[22] may possibly allow one to extend the torque theory to the case of the hybrid wire, as it does for nickel wires containing a domain wall.[43] However, the case of the homogeneous nickel wire, where the current is thought to enter unpolarized but exit the wire polarized, may require different assumptions.

An explanation was suggested, different than torque theory, for the angular dependence of $\triangle H_{\max}(\Omega)$ applicable to *both* the homogeneous nickel wires and hybrid wires.[21] The spin interaction taking place between the probe and the current is viewed as an out of equillibrium thermokinetic

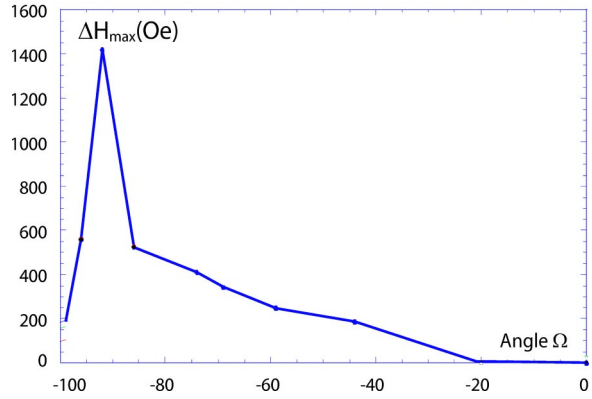

FIG. 19. (Color online). Measured angular dependence of the parameter $\Delta H_{\max}$ for a nickel half wire with Spin polarizer made of 15 cobalt layers grown with the single bath technique. The sample exhibits well separated GMR and AMR.

balance between spin interactions and the change in magnetization orientation.[21,52] In that model the angular momentum carried by conduction electrons is partially transferred to localized ferromagnetic moments in a diffusive way (in the sense that the spins are modified at collision sites in the ferromagnet), thus the transfer takes place at the interface of electrons entering the magnet on the length scale of the spin-diffusion length. The generalized Landau-Lifshitz equation with the additional term describing the change in the magnetization due to the spin-flip scattering inside the magnet can be written in that model with $\vec{f}(\vec{e_p}) = \beta(p/L)\vec{e_p}$ where β is the spin-polarization ratio of the electrons at the fermi level, L is the length of the wire and p is a geometric factor close to 1.[21] This model gives

$$\frac{d\vec{M}}{dt} \approx -g' M_s \left(\vec{M}_0 \times \frac{dV}{d\vec{M}_0} \right) - h' \left(\vec{M}_0 \times \frac{dV}{d\vec{M}_0} \right) \times \vec{M}_0 + p \frac{g \mu_B \beta I_p \vec{e}_p}{eL}, \tag{11}$$

where $\vec{M}_0$ is the magnetization of the wire without the current and I_p is always positive (whatever the current sense).

From Eq. (9) at steady state (just before the irreversible jump), one can get $\Delta h(\Omega, \varphi)$ by specifying the potential energy $V(\Omega, \varphi; h)$. For a uniformly magnetized nanowire with uniaxial anisotropy $\Delta h_{\max}(\Omega) = \Delta h(\Omega, \varphi = \varphi_c)$ is then given by[21]

$$\Delta h_{\max} = h_{\mathrm{sw}}(\Omega) - \frac{2cI_p \ (\vec{e}_p \cdot \vec{v}) - \sin(2\varphi_c)}{\sin(\varphi_c - \Omega)}, \tag{12}$$

where φ_c is the angle the magnetization makes with the wire axis at $h - \triangle h_{\max}$ during pulse injection, $\vec{v}$ is the polar vector perpendicular to $\vec{M}$, the parameter c is phenomenological and depends on the spin-polarization rate and on the Gilbert damping parameter.

To fit the data $\triangle h_{max}(\Omega)$, the most direct way to do it is to take the experimental values of h_{sw} and extracting the angle φ_c from the fits of $R(H)$ in terms of uniform rotation of magnetization. Since the theoretical curve uses experimental values of h_{sw} it also has scatter. An additional scattering of the curve can also occur due to the sensitivity of the estimation of $\triangle h$ in errors on φ_c through the term $\sin(\varphi_c - \Omega)$. It can be seen that the theory accounts for the main feature of the data (Fig. 20).

VII. CONCLUSIONS

It could be shown that the injection of an electrical current of high density ($j_p \approx 10^7$ A/cm^2)in a nickel wire near a metastable state provokes the transition from an equilibrium state onto another equilibrium state that can also be reached by a minor field sweep without pulse injection (making a minor hysteresis loop). Conversely, if a minor loop does not exhibit a hysteresis, the pulse does not provoke an observable transition.

The presence of a source of spin polarization (cobalt

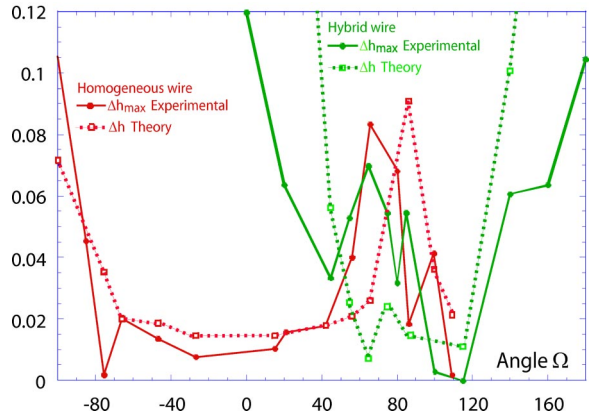

FIG. 20. (Color online). Experimental vs predicted values for $\triangle h_{\max}(\Omega)$ produced by a negative current flow by taking a parameter $c=200$ for the homogeneous wire and $c=155$ for the hybrid wire.

layer)—at a distance to the nickel wire smaller than typical spin transport length scales—modifies the current-induced effect on the magnetic state of a nickel probe in a way that can be linked only to the spin polarization of the injected current. Indeed, the difference in angular dependence (angle the applied field makes with the wire axis) of the current-induced effect between a nickel wire and a hybrid wire containing a nickel half wire (of similar properties to the nickel wire alone) clearly relates the effect to the presence of the multilayer half wire in the hybrid wire. That multilayer serves as a conduction-electron spin polarizer. This excludes possible causes to the effect such as the Joule heating, the current-induced Oersted field or its gradient, or the addition of their contributions, which do not depend on the presence of the multilayer.

Joule heating may be excluded for three reasons. First the presence of asymmetries in sense of current. The thermal power dissipated does not depend on current sense whatever the magnetic configurations. Second, the study of $\triangle H_{\max}$ as a function of the wire diameter at constant current $I=1$ mA, has shown that the maximum of $\triangle H_{\max}$ of about 800 Oe for ≈ 40 nm radius decreases to 300 Oe for ≈ 15 nm radius. Third, time-resolved measurements of the increase in resistance during pulse injection, are consistent with theoretical estimations of about 10 K, which accounts only for a 30 Oe variation of the switching field (not shown).

The effect of the current-induced Oersted field can also be excluded. $\text{Max}\triangle H_{\max}$ at fixed current intensity decreases with diameter, in the range of diameters lower than $r \approx 35$ nm. This is contradictory with the increase of the current-induced Oersted field as the wire is reduced and the current intensity is kept constant. Also, in the range of diameters above $r \approx 35$ nm the amplitude of the current-induced Oersted field becomes quite lower than $\max\triangle H_{\max}$, making of the current-induced Oersted field an unlikely substantial contributor to $\max\triangle H_{\max}$ in the said range of wire radii.

Finally, the gradient of the current-induced Oersted field must also be excluded. The gradient of the current-induced Oersted field is more than one order of magnitude lower than the gradient in field in a typical domain wall in nickel. Hence no domain wall is created that could propagate and thus produce the magnetization reversal.

ACKNOWLEDGMENT

This work was done with the help of the Swiss National Science Foundation Grant No. 20-63460.00.

*Present address: Nanocenter Basel and Institute of Physics, Klingelbergstrasse 82, CH-4056 Basel, Switzerland.
†Present address: Ecole Polytechnique, Laboratoire des solides irradiés 91128 Palaiseau Cedex, France.
‡ URL http://ipewww.epfl.ch/gr_ansermet/ansermet_welcome.html

[1] A.H. Mitchell, Phys. Rev. **105**, 1439 (1957).
[2] A. Fert and I.A. Campbell, Phys. Rev. Lett. **21**, 1190 (1968).
[3] C. Kittel and A.H. Mitchell, Phys. Rev. **101**, 1611 (1956).
[4] M. Johnson and R.H. Silsbee, Phys. Rev. Lett. **55**, 1790 (1985).
[5] M. Johnson and R.H. Silsbee, Phys. Rev. B **35**, 4959 (1987).
[6] M.N. Baibich, J.M. Broto, A. Fert, F. Nguyen Van Dau, F. Petroff, P. Etienne, G. Creuzet, A. Friederich, and J. Chazelas, Phys. Rev. Lett. **61**, 2472 (1988).
[7] G. Binasch, P. Grünberg, F. Saurenbach, and W. Zinn, Phys. Rev. B **39**, 4828 (1989).
[8] M.A.M. Gijs and G.E.W. Bauer, Adv. Phys. **46**, 285 (1997).
[9] J.S. Moodera, L.R. Kinder, T.M. Wong, and R. Meservey, Phys. Rev. Lett. **74**, 3273 (1995).
[10] J.-Ph. Ansermet, J. Phys.: Condens. Matter **10**, 6027 (1998).
[11] G. Tatara, Y.-W. Zhao, M. Munoz, and N. Garcia, Phys. Rev. Lett. **83**, 2030 (1999).
[12] R.P. van Gorkom, A. Brataas, and G.E.W. Bauer, Phys. Rev. Lett. **83**, 4401 (1999).
[13] J.F. Gregg, W. Allen, K. Ounadjela, M. Viret, M. Hehn, S.M. Thompson, and J.M.D. Coey, Phys. Rev. Lett. **77**, 1580 (1996).
[14] P.M. Levy and S. Zhang, Phys. Rev. Lett. **79**, 5110 (1997).
[15] J.-E. Wegrowe, A. Comment, Y. Jaccard, J.-Ph. Ansermet, N.M. Dempsey, and J.P. Nozières, Phys. Rev. B **61**, 12 216 (2000).
[16] J.C. Sloncewski, J. Magn. Magn. Mater. **159**, L1 (1996).
[17] J.C. Sloncewski, J. Magn. Magn. Mater. **195**, L261 (1999).
[18] L. Berger, Phys. Rev. B **54**, 9353 (1996).
[19] L. Berger, J. Appl. Phys. **81**, 4880 (1997).
[20] L. Berger, J. Appl. Phys. **55**, 1954 (1984).
[21] J.-E. Wegrowe, Phys. Rev. B **62**, 1067 (2000).
[22] Y.B. Bazaliy, B.A. Jones, and S.-C. Zhang, Phys. Rev. B **57**, R3213 (1998).
[23] Y.B. Bazaliy, B.A. Jones, and S.-C. Zhang, J. Appl. Phys. **89**, 6793 (2001).
[24] E. Sahli and L. Berger, J. Appl. Phys. **76**, 4787 (1994).
[25] J.Z. Sun, Phys. Rev. B **62**, 570 (2000).
[26] X. Waintal, E.B. Myers, P.W. Brouwer, and D.C. Ralph, Phys. Rev. B **62**, 12 317 (2000).
[27] K. Xia, P.J. Kelly, G.E.W. Bauer, A. Brataas, and I. Turek, Phys. Rev. B **65**, 220401 (2002).
[28] C. Heide, P.E. Zilberman, and R.J. Elliott, Phys. Rev. B **63**, 064424 (2001).
[29] S. Zhang, P.M. Levy, and A. Fert, Phys. Rev. Lett. **88**, 236601 (2002).
[30] P.P. Freitas and L. Berger, J. Appl. Phys. **57**, 1266 (1985).
[31] C.Y. Hung and L. Berger, J. Appl. Phys. **63**, 4276 (1988).

[32] N. Garcia, H. Rohrer, I.G. Saveliev, and Y.-W. Zhao, Phys. Rev. Lett. **85**, 3053 (2000).
[33] N. Garcia, I.G. Saveliev, Y.-W. Zhao, and A. Zlatkine, J. Magn. Magn. Mater. **214**, 7 (2000).
[34] M. Tsoi, A.G.M. Jansen, J. Bass, W.C. Chiang, M. Seck, V. Tsoi, and P. Wyder, Phys. Rev. Lett. **80**, 4281 (1998).
[35] M. Tsoi, A.G.M. Jansen, J. Bass, W.C. Chiang, V. Tsoi, and P. Wyder, Nature (London) **406**, 46 (2000).
[36] S.M. Rezende, F.M. de Aguiar, M.A. Lucena, and A. Azevedo, Phys. Rev. Lett. **84**, 4212 (2000).
[37] S.J.C.H. Theeuwen, J. Caro, K.P. Wellock, S. Radelaar, C.H. Marrows, B. Hickey, and V.I. Kozub, J. Appl. Phys. **75**, 3677 (1999).
[38] J.Z. Sun, J. Magn. Magn. Mater. **202**, 157 (1999).
[39] J.A. Katine, F.J. Albert, R.A. Buhrman, E.B. Myers, and D.C. Ralph, Phys. Rev. Lett. **84**, 3149 (2000).
[40] E.B. Myers, D.C. Ralph, J.A. Katine, R.N. Louie, and R.A. Buhrman, Science **285**, 867 (1999).
[41] J. Grollier, V. Cros, A. Hamzic, J.M. Georges, H. Jaffrès, A. Fert, G. Faini, J. Ben Youssef, and H. Le Gall, Appl. Phys. Lett. **78**, 3663 (2001).
[42] W. Weber, S. Riesen, and H.C. Siegmann, Science **291**, 1015 (2001).
[43] J.-E. Wegrowe, D. Kelly, Y. Jaccard, Ph. Guittienne, and J.-Ph. Ansermet, Europhys. Lett. **45**, 626 (1999).
[44] J.-E. Wegrowe, S. E. Gilbert, D. Kelly, B. Doudin, and J.-Ph. Ansermet, IEEE Trans. Magn. **34**, 903 (1998).
[45] A. Aharoni, J. Appl. Phys. **30**, 705 (1959).
[46] Y. Jaccard, Ph. Guittienne, D. Kelly, J.-E. Wegrowe, and J.-Ph. Ansermet, Phys. Rev. B **62**, 1141 (2000).
[47] J. Meier, B. Doudin, and J.-Ph Ansermet, J. Appl. Phys. **79**, 6010 (1996).
[48] Ch. Schönenberger, B.M.I Van Der Zande, L.G.J. Fokkink, M. Henny, C. Schmid, M. Krüger, A. Bachtold, R. Huber, H. Birk, and U. Staufer, J. Phys. Chem. B **101**, 5497 (1997).
[49] A. Blondel, J.-P. Meier, B. Doudin, and J.-Ph Ansermet, Appl. Phys. Lett. **65**, 3019 (1994).
[50] A. Blondel, J. Meier, B. Doudin, J.-Ph Ansermet, K. Attenborough, P. Evans, R. Hart, G. Nabiyouni, and W. Schwarzacher, J. Magn. Magn. Mater. **148**, 317 (1995).
[51] J.-E. Wegrowe, D. Kelly, A. Franck, S. E. Gilbert, and J.-Ph. Ansermet, Phys. Rev. Lett. **82**, 3681 (1999).
[52] J.-E. Wegrowe, D. Kelly, Ph. Guittienne, and J.-Ph. Ansermet, Europhys. Lett. **56**, 748 (2001).
[53] J.-E. Wegrowe, X. Hoffer, D. Kelly, Ph. Guittienne, and J.-Ph. Ansermet, J. Appl. Phys. **89**, 7127 (2001).
[54] A similar argument was also suggested by J.Z. Sun in his numerical study of a spin-polarized current acting on a monodomain magnet with anisotropies, where he mentioned the sensitivity of the polarization ratio to the quality of the interface (Ref. 25).
[55] J. Meier, Ph.D. thesis, EPFL, Switzerland, 1997.
[56] D. Kelly, Ph.D. thesis, EPFL, Switzerland, 2001.
[57] Ph. Guittienne, J.-E. Wegrowe, D. Kelly, and J.-Ph. Ansermet, IEEE Trans. Magn. **37**, 2126 (2001).
[58] J.-E. Wegrowe, A. Fabian, X. Hoffer, Ph. Guittienne, D. Kelly, E. Olive, and J.-Ph. Ansermet, Appl. Phys. Lett. **80**, 3775 (2002).
[59] W.T. Coffey, Yu.P. Kalmykov, and J.T. Waldron, *The Langevin Equation*, Vol. 11 of World Scientific Series in Contemporary Chemical Physics (World Scientific, Singapore, 1996), p. 337.